International Journal of Nanomedicine

Dovepress

open access to scientific and medical research

Open Access Full Text Article

ORIGINAL RESEARCH

Rosuvastatin Nanomicelles Target Neuroinflammation and Improve Neurological Deficit in a Mouse Model of Intracerebral Hemorrhage

Liu Zi,[1,2,*] Wencheng Zhou,[1,3,*] Jiake Xu,[1,4] Junshu Li,[5] Ning Li,[2] Jianguo Xu,[1,4,6] Chao You,[1,4,6] Chengwei Wang,[1,2] Meng Tian[1,4,6]

[1]Neurosurgery Research Laboratory, National Clinical Research Center for Geriatrics, West China Hospital, Sichuan University, Chengdu, Sichuan, People's Republic of China; [2]Department of Integrated Traditional and Western Medicine, West China Hospital, Sichuan University, Chengdu, Sichuan, People's Republic of China; [3]Department of Burn and Plastic Surgery, West China Hospital, Sichuan University, Chengdu, Sichuan, People's Republic of China; [4]Department of Neurosurgery, West China Hospital, Sichuan University, Chengdu, Sichuan, People's Republic of China; [5]State Key Laboratory of Biotherapy and Cancer Center, West China Hospital, Sichuan University and Collaborative Innovation Center for Biotherapy, Chengdu, Sichuan, People's Republic of China; [6]West China Brain Research Centre, West China Hospital, Sichuan University, Chengdu, Sichuan, People's Republic of China

*These authors contributed equally to this work

Correspondence: Chengwei Wang; Meng Tian
Neurosurgery Research Laboratory, National Clinical Research Center for Geriatrics, West China Hospital, Sichuan University, No. 37 Guoxue Alley, Wuhou District, Chengdu, Sichuan Province, 610041, People's Republic of China
Tel/Fax +86 28 85164168
Email 21270526@qq.com; tianmong007@gmail.com

Background: Intracerebral hemorrhage (ICH), a devastating subtype of stroke, has a poor prognosis. However, there is no effective therapy currently available due to its complex pathological progression, in which neuroinflammation plays a pivotal role in secondary brain injury. In this work, the use of statin-loaded nanomicelles to target the neuroinflammation and improve the efficacy was studied in a mouse model of ICH.

Methods: Rosuvastatin-loaded nanomicelles were prepared by a co-solvent evaporation method using polyethylene glycol-poly(ε-caprolactone) (PEG-PCL) copolymer as a carrier. The prepared nanomicelles were characterized by transmission electron microscopy (TEM) and dynamic light scattering (DLS), and then in vitro and in vivo studies were performed.

Results: TEM shows that the nanomicelles are spherical with a diameter of about 19.41 nm, and DLS shows that the size, zeta potential, and polymer dispersity index of the nanomicelles were 23.37 nm, −19.2 mV, and 0.221, respectively. The drug loading content is 8.28%. The in vivo study showed that the nanomicelles significantly reduced neuron degeneration, inhibited the inflammatory cell infiltration, reduced the brain edema, and improved neurological deficit. Furthermore, it was observed that the nanomicelles promoted the polarization of microglia/macrophages to M2 phenotype, and also the expression of the proinflammatory cytokines, such as IL-1β and TNF-α, was significantly down-regulated, while the expression of the anti-inflammatory cytokine IL-10 was significantly up-regulated. The related mechanism was proposed and discussed.

Conclusion: The nanomicelles treatment suppressed the neuroinflammation that might contribute to the promoted nerve functional recovery of the ICH mouse, making it potential to be applied in clinic.

Keywords: rosuvastatin, nanomicelles, neuroinflammation, intracerebral hemorrhage

Introduction

Intracerebral hemorrhage (ICH) is a devastating form of stroke that has a poor prognosis where the mortality of the patients was 40.4% in the first month and only 12–39% of survival could regain the life self-care ability.[1,2] However, effective therapy is currently absent due to its complex pathological progression mainly including two phases: a primary injury and followed by a much more complicated secondary injury.[3] In these mechanisms, inflammatory cascade reactions closely related to injury progressions, such as microglia activation, the release of

inflammatory cytokines, and necrosis of nerve cells, play a key role in clinical outcomes. Therefore, the inflammatory response can be considered as one of the most critical and basic targets for the overall prognosis of intracerebral hemorrhage.[4]

Statins are considered to be competitive inhibitors of 3-hydroxyl-3-methylglutaryl coenzyme A reductase (HMGCR). They are not only used to reduce low-density lipoprotein (LDL) cholesterol and prevent cardiovascular diseases but also play a role in many other conditions, including inhibiting inflammatory reaction, antioxidants, improving endothelial function, and even inhibiting mitosis of cancer cells.[5–8] For example, statin was identified as a potential neuroprotective agent that targeted the inflammatory response following ICH. However, the use of statin was usually limited by its inherent drawbacks. First, it is poorly water-soluble that results in poor absorption, and low bioavailability via oral administration.[9] Second, the high-dose of statin has been thought to have led to numerous complications, such as increased myopathy/myalgia and increased risk of ICH and diabetes mellitus.[10–12] Thus, there has been great interest in using an effective drug delivery system for statins to improve its efficiency.[13,14] In this regard, the nano-drug delivery system has great promise as it effectively extends the half-life of the drug's cycle and allows for the administration of lower doses and at a lower frequency to minimize toxicity.[15–17] Specifically, polymeric nanomicelles that self-assemble from copolymers composed of a hydrophilic shell and a hydrophobic core are good candidates for poorly water-soluble or hydrophobic drugs where the drugs stay in the core and the hydrophilic shell provides a stabilizing interface between the core and the outside aqueous environment.[18–20] For instance, poly (ethylene glycol)-block-poly (ε-caprolactone) (PEG-PCL) copolymers have been widely used in a nano-drug delivery system, since they are biocompatible, nontoxic, and not accumulative in vivo because the degradation products of the copolymers can enter the tricarboxylic acid cycle or be eliminated by the kidney, and therefore the nanomicelles formed from the PEG–PCL copolymers have attracted more and more interesting in various drug delivery system.[21–23] There is a current lack of information about statins loaded nanomicelle for ICH treatment.

In this work, the possibility of using nanomicelles to deliver statin to improve its efficacy in ICH was explored. We hypothesized that the statin-loaded nanomicelles were capable of targeting the neuroinflammation in ICH and thus promoting the nerve functional recovery. To address this hypothesis, as shown in Figure 1A, the rosuvastatin-loaded nanomicelles were first prepared and characterized, and then the efficacy of the nanomicelles was investigated in a mouse model of ICH (Figure 1B), including behavior test, brain water content, examination of histology, immunohistochemistry, immunofluorescence, and Western blot.

Materials and Methods

Materials

Rosuvastatin was obtained from Solarbio (IR0150, Solarbio, Beijing, China). Poly (ethylene glycol) 2000-block-poly(ε-caprolactone) 3000 (PEG-PCL) was purchased from Shanghai ToYongBio Tech. Inc. (Shanghai, China). Fluoro-Jade C dyestuff was obtained from Merck (AG325-30MG, Millipore, Darmstadt, Germany). Rabbit anti-iNOS, rabbit anti-β-Tublin and mouse anti-Arginase 1 were purchased from Proteintech (1895-1-AP, 10094-1-AP, 66129-1-Ig, Proteintech, Wuhan, China). Goat anti-Iba-1 were purchased from Wako Pure Chemical Industries (011-27991, Wako, Osaka, Japan). Rabbit anti-IL-1β was supplied from Abbkine (ABP52932, Abbkine, Redlands, California). Rabbit anti- TNF-α was purchased from HuaAn Biotechnology (ER1919-22, HuaAnBio, Hangzhou, China). Rabbit anti- IL-10 was supplied from Wanleibio (WL03088, Wanleibio, Shenyang, China) Fluorescent Alexa 488 and 555 were purchased from Invitrogen (A-21121, A-11008, A-21432, Invitrogen, CA, USA). Peroxidase AffiniPure Goat Anti-Mouse IgG (H+L), AffiniPure Goat Anti-Rabbit IgG (H+L) were purchased from Jackson (115-035–003, 111-005-003, Jackson ImmunoResearch, PA, USA). The secondary antibodies for WB were goat anti-mouse IgG-HRP and goat anti-rabbit IgG-HRP (ZB-2301; ZB-2305; Zhongshan Golden Bridge, Beijing, China).

Preparation of Statin-Loaded Nanomicelles

The rosuvastatin-loaded nanomicelles were prepared by a co-solvent evaporation method.[24] In short, PEG-PCL copolymer (50 mg) and rosuvastatin (5 mg) were dissolved into tetrahydrofuran (500 μL) and then infused into distilled water (5 mL) at a stirring rate of 200 rpm using magnetic stirring. The solution was vigorously stirred at 25°C for 24 h to fully extract the solvent using a co-solvent evaporation process, and a sufficient amount of distilled water was supplemented to keep the volume to

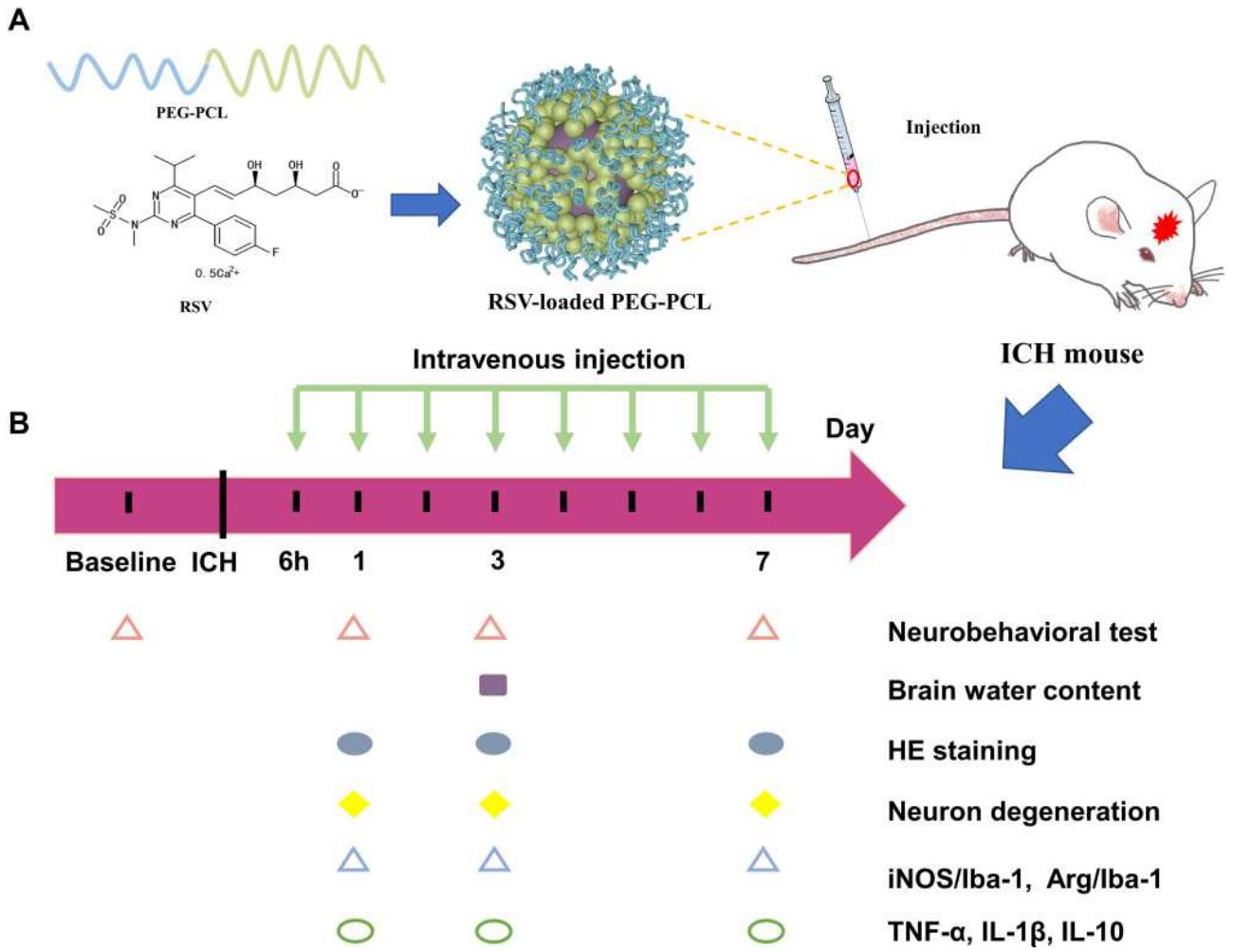

Figure 1 (**A**) Schematic presentation of rosuvastatin-loaded nanomicelles injection into an ICH mouse. (**B**) Experimental protocol and timeline.

5 mL to obtain nanomicelles with a concentration of 10 mg/mL. After filtered via a 0.45 μm filter, the final solution was stored for further use at 4°C. The drug loading content (DLC) of the nanomicelles was determined by ultraviolet spectroscopy at 243 nm and the percentage of DLC was estimated by formula (1):

$$DLC(\%) = \frac{amount\ of\ drug\ in\ micell}{amount\ of\ drug\ -\ loaded\ micell} \times 100\% \quad (1)$$

Characterization of the Nanomicelles

The size, zeta potential, and polymer dispersity index (PDI) were examined by NanoBrook Omni particle size and zeta potential analyzer (Brookhaven, New York, USA). Transmission electron microscopy (TEM; Hitachi HT7700, Japan) was used to determine the morphology of nanomicelle.

Cytotoxicity Assay

The mouse embryonic fibroblast (NIH/3T3) cell line, purchased from Type Culture Collection of Chinese Academy of Sciences (Shanghai, China), was used to test the cytotoxicity of the nanomicelles. The cells were cultured under conventional conditions as previously described.[25] The cells in the logarithmic phase were collected and the concentration of the cell suspension was adjusted. A total of 100 μL of cell suspension was added into each well of a 96-well plate to make the cell density to 2000/well. After 24 hours of cell culture, 10 μL of three concentrations (1, 0.5, and 0.1 mg/mL) of nanomicelles were added into each well, with 5 repeated wells in each concentration while five wells were served as blank control without nanomicelles. After further culture for 24, 48, and 72 hours, the CCK-8 kit was used to detect the cytotoxicity. At each set time, the CCK-8 agent (10 μL) was added into each well. After incubation for 1 hour, the absorbance was measured

at 450 nm. The cytotoxicity was expressed by the ratio of absorbance between the experimental group and the control group.

In vitro Macrophage Cells Culture with Nanomicelles

Mouse macrophage cell line RAW 264.7 was purchased from Type Culture Collection of Chinese Academy of Sciences (Shanghai, China), and cultured in DMEM with 10% FBS. The RAW 264.7 macrophage cells were seeded in a 24-well plate with cell-climbing slices and incubated overnight at 37°C. Cells were pretreated for 6 h with (i) Rosu-nano (containing 1000 ng/mL), (ii) Rosu alone at 1000 ng/mL and (iii) vehicle control (cell medium alone), washed with PBS and then stimulated with 100 ng/mL lipopolysaccharide (LPS) (Sigma–Aldrich, MO, USA) and 100 ng/mL interferon-γ (IFN-γ, Thermo Fisher Scientific) for 18 h. Cells on the slides were fixed with 4% paraformaldehyde (PFA)/PBS for 10 min. Primary antibody (anti-iNOS and anti-ARG–1) was added and incubated for an hour at room temperature; then, the second antibody was added and incubated at room temperature for 30 min.

Animal

Animal experiments were performed in accordance with the Chinese National Guidelines for the Use and Care of Experimental Animals, approved by the Animal Ethical Committee West China Hospital, Sichuan University (NO. 2020405A). For the study, Kunming (KM) mice were used (2–3 months age and weighing 22–28 g, Dashuo Laboratory Animal Co. Ltd., China). The mice had been housed under controlled conditions in a special pathogen-free lab at the animal center of West China Hospital, Sichuan University (12-hour dark-light cycle, controlled temperatures and moisture, and free access to food and water). Efforts were made to minimize animal suffering.

ICH Modeling

Mice were anesthetized with pentobarbital (40 mg/kg) and put in a stereotactic frame (68001; RWD Life Science Co., Ltd., Shenzhen, China). The skull was extensively exposed after skin incisions, and a small hole was drilled into the skull (coordinates: 0.8 mm anterior, 2.0 mm lateral, and 2.9 mm ventral to the bregma). Then, 0.075 units Collagenase VII (0.075 Units in 0.5 μL saline; Sigma, St. Louis, MO) were injected into the right striatum using a 1 μL Hamilton syringe. The opening was filled using bone wax.

Experimental Groups and Pharmacological Interventions

Animals were randomly divided into 3 groups after modeling (Rosuvastatin group, Nanomicelle group, and Vehicle group), and, respectively, treated with rosuvastatin (1 mg/kg) by oral administration, rosuvastatin-loaded nanomicelles (1 mg/kg) by tail intravenous injection, and saline by tail intravenous injection. The statin dosage was selected based on earlier studies.[26] The mice were treated at 6 hours after surgery and then daily for up to 7 days.

Neurobehavioral Testing

As previously mentioned, a 28-point neurologic deficit scale (NDS) was used to assess neurologic deficits, including body symmetry, gait, climbing, circling behavior, front limb symmetry, compulsory circling, and whisker response.[27,28] Mice (n=6 per group) were tested for three consecutive days before operation to exclude abnormal mice and form baseline data. And NDS was measured on days 1, 3, and 7 after ICH. The scoring was performed in a blinded fashion by two experimenters.

Measurement of Brain Water Content

Brain water content was measured at 72 hours after surgery as previously reported.[29] Briefly, mice (n=6 per group) were decapitated under lethal isoflurane anesthesia and brains were quickly removed. A coronal brain section of 4 mm thickness was separated 2 mm anterior and posterior of the needle tract, and then further divided into ipsilateral and contralateral cortex and basal ganglia. The cerebellum was additionally collected as an internal control. All brain specimens were weighed using an analytical microbalance (QUINTIX35-1CN, Sartorius, Beijing, China) in order to obtain the wet weight. Samples were then dried at 100°C for 24 hours before determining the dry weight. The brain water content (%) was calculated as (wet weight– dry weight)/wet weight × 100%.

Histology and Immunostaining

Histological Treatment

Mice (n=4 per group) were deeply anesthetized and transcardially perfused with 10% paraformaldehyde (PFA). The brains were removed and fixed for 24 hours in 10% formalin, and then cut as a slice of appropriate size. Following,

tissues were dehydrated and paraffin-embedded. Paraffin blocks were trimmed into coronal sections (4 μm-thick) with a microtome (Leica RM2235, Germany).

Hematoxylin and Eosin (H&E) Staining

Using regular methods, paraffin blocks were stained with H&E. All stained sections have been visualized and photographs have been digitally collected using a ZEISS light microscope (Axioplan 2, Carl Zeiss MicroImaging GmbH, Germany) for further histological study.

Fluoro-Jade C (FJC) Staining

Degenerating neurons were assayed by FJC staining as previously described[30] In each section, the number of FJC-positive cells was counted manually.

Immunofluorescence Staining

After dewaxing the paraffin sections of brain tissue, antigen retrieval was performed by incubating the sections in retrieval buffer at 100°C for 24 min. Sections were then blocked in 5% natural serum. Subsequently, all sections were incubated overnight with primary antibodies to iNOS (1:200 dilution) or Iba-1 (1:500 dilution) or Arginase-1 (1:200 dilution) at 4°C. After washing, adding corresponding secondary antibodies for 1 h at room temperature. A fluorescence microscope (AX10 imager A2/AX10 cam HRC; Carl Zeiss, Germany) was used to observe the results.

Immunohistochemical Staining

The preceding steps were identical to those used for tissue immunofluorescence. Following that, brain sections were incubated for 15 min at room temperature into a mixed solution (3% H2O2). After incubation with mouse anti-IL-1β (1:100 dilution) or TNF-α (1:100 dilution) at 4°C overnight, the sections were incubated at 37°C with biotin-tagged goat anti-mouse IgG for 30 min and then blocked at 37°C for 1 h at 5% bovine serum albumin. Lastly, the sections were colored with diaminobenzidine, followed by hematoxylin. A ZEISS light microscope has observed the pictures (Axioplan 2, Carl Zeiss MicroImaging GmbH, Germany). Open-source program ImageJ/Fiji (US National Institutes of Health, https:/imagej.nih.gov/ij/) measured the positive areas of TNF-α and IL-1β.

Western Blot

Ipsilateral brain tissues (both hematomal and perihematomal brain regions) were homogenized with Precellys 24 dual tissue homogenizer (Bertin Technologies, Montigny-le-Bretonneux, France). RIPA buffer containing protease and phosphatase inhibitors was added and incubated for 30 min on ice. After sample preparation, equal amounts of protein were loaded onto an SDS-PAGE gel to have the electrophoresis. After protein separation, the gel was covered with a PVDF membrane for protein transfer. Subsequently, the membrane was blocked for 2 h at room temperature and incubated overnight at 4°C with the following primary antibodies: anti-iNOS (1:1000), anti-ARG1 (1:20000), anti-IL-1β (1:1000), anti-TNF-α (1:1000), anti-IL-10 (1:1000), anti-β-Tublin (1:30000). The secondary antibodies were all from Zhongshan Golden Bridge Biotechnology. Image J/Fiji software was used to analyze the gray value of the Western blot.

Statistical Analysis

Two researchers have carried out all the work in a blind manner. All statistics have been computed using SPSS program (SPSS Inc., Chicago, IL, USA). One-way ANOVA followed by Tukey's multiple comparison test was used to assess whether there was a significant difference between three groups of samples. Differences at $P < 0.05$ were considered significant.

Results and Discussion

Preparation and Characterization of Rosuvastatin-Loaded Nanomicelles

Rosuvastatin is a synthetic, high potent second-generation statin used for the management of high cholesterol levels and related conditions.[31] However, like other types of statin, rosuvastatin is lipophilic and has an oral bioavailability of only 20% due to its poor aqueous solubility. PEG-PCL is an amphiphilic copolymer that could self-assemble into nanomicelles, in which the PCL block is capable of forming a hydrophobic core to hold the desired payload with hydrophobicity, and the PEG block is hydrophilic to form an outside shell, and thus the PEG-PCL nanomicelles could increase the solubility of hydrophobic drugs by encapsulation them in the core. Herein, we used the PEG-PCL copolymer to prepare rosuvastatin-loaded nanomicelles by a co-solvent evaporation method. The UV absorption of rosuvastatin is 243 nm, and the DLC was 8.28%. The morphology of the micelles was observed by TEM. Figure 2A shows that the micelles are spherical with a diameter of about 19.41 nm. The size, zeta potential, and PDI of the micelles were determined by DLS and the results were 23.37 nm (Figure 2B), −19.2 mV, and 0.221, respectively. The size of the nanomicelles determined by TEM was smaller than that in DLS determination because

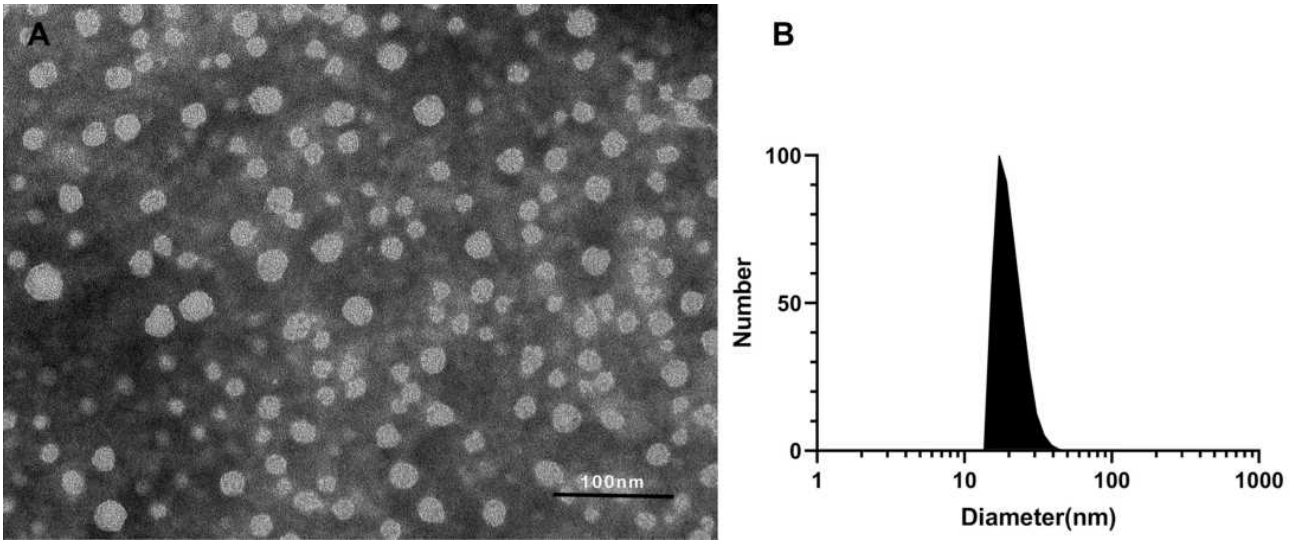

Figure 2 Characterization of rosuvastatin-loaded nanomicelles. (**A**) TEM image of rosuvastatin-loaded nanomicelles, scale bar = 100 nm. (**B**) Particle sizes of rosuvastatin-loaded nanomicelles detected by DLS.

of the different determination conditions where TEM operation in the dry state while DLS operation in the wet state.

Cytotoxicity of Nanomicelles

The cytotoxicity of the nanomicelles was assayed by the CCK8 kit before animal experiments. The cell viability of the samples at all concentrations maintained more than 85% at all time points (Figure 3). With the increase of the micellar concentration, the cytotoxicity was not obvious. Moreover, with the extension of culture time, the micelles did not damage the cell viability. The results of the cytotoxicity test confirmed the safety of the micelles for subsequent in vivo experiments.

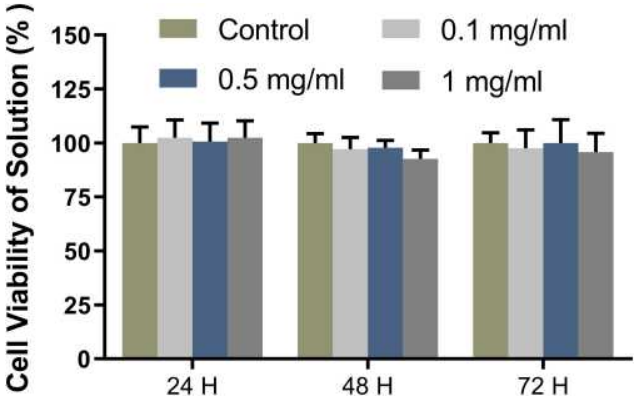

Figure 3 Cytotoxicity of the nanomicelles with different concentrations. The ratio of the sample absorbance to that of the blank control group presents the cell viability rate.

Neurological Deficits and Brain Edema

To determine whether nanomicelles improve motor and sensory function after nerve damage, we subjected the mice to a battery of behavior tests at 1, 3, and 7 day. As shown in Figure 4A, all groups showed the same baseline (Pre-ICH) and displayed similar neurological impairments at 24 h after ICH where the mice demonstrated marked focal contralateral motor deficits. With the time prolonged, the animals demonstrated some recovery of function as previous reports.[32,33] For the Rosuvastatin group, there was a similar trend of the neurological deficit as the Vehicle group. In contrast, on both days 3 and 7, the mice in nanomicelle group decreased the neurological deficit score compared with those in the vehicle group ($P < 0.05$) and rosuvastatin group ($P < 0.05$).

Brain edema was evaluated at 72 hours after surgery. Treated mice with nanomicelles showed a significantly reduced brain water content in the basal ganglia and cortex ($p<0.05$, compared to vehicle, Figure 4B). More importantly, brain edema in the nanomicelle group was attenuated significantly in the ipsilateral basal ganglia ($p<0.05$, compared to rosuvastatin).

Neurological deficits are well-known clinical endpoints for ICH trials. In rats and mouse models of unilateral brain injury, including cerebral ischemia[34] and ICH,[35] various tests were used to determine acute neurological function changes. In our model, the animals were scored neurologically for focal deficits at 1, 3, and 7 days using a 28-

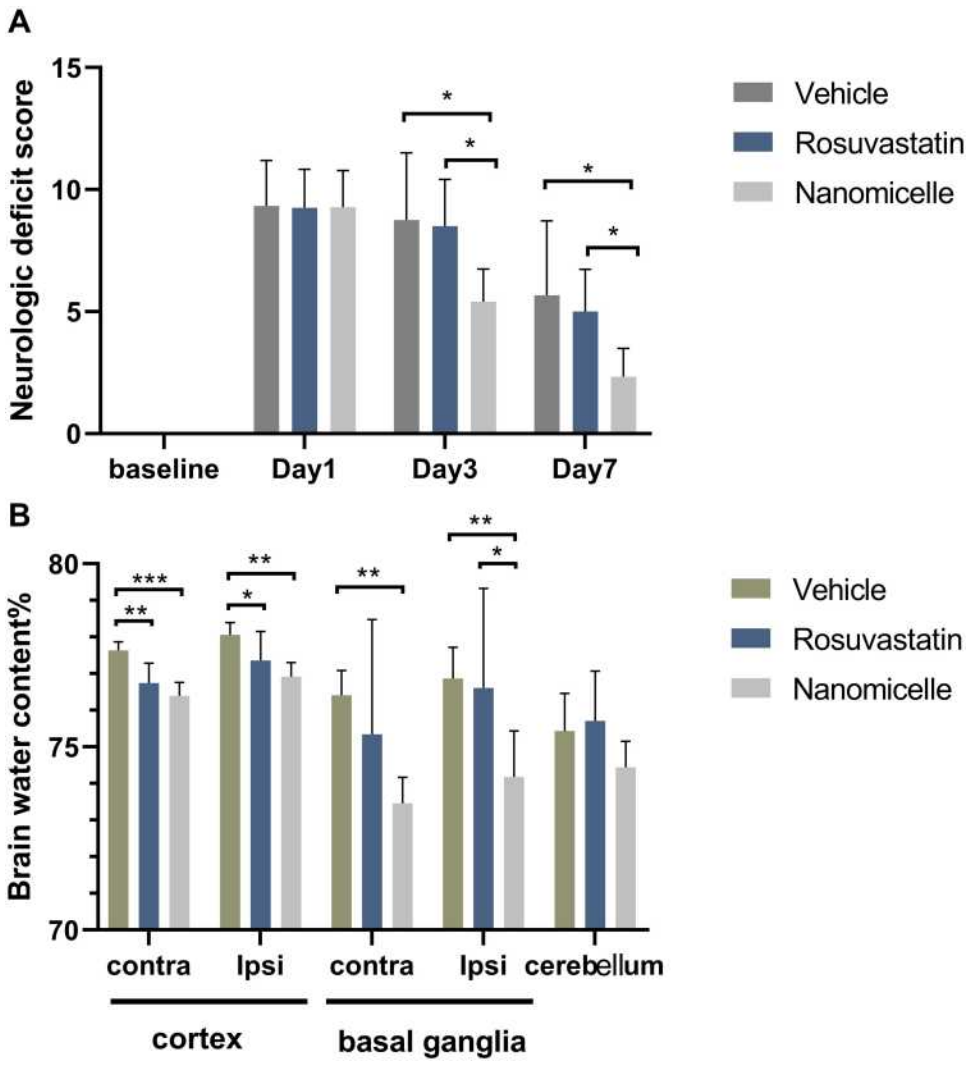

Figure 4 Neurological deficits and brain edema. (**A**) Neurological deficit score after ICH. (**B**) Percentage of brain water content. Data are shown as mean ± SD (n = 6), *P < 0.05, **P<0.01, ***P < 0.001.

point neurological score system that is sensitive to neurological deficits after injury. Oral administration of statin exhibited a similar trend of the neurological deficit as the saline control, indicating that there was no efficacy in the case of oral administration. When using the nanomicelles, a significant improvement in the neurological deficit was observed, suggesting that the nanomicelles have better efficacy than that of oral administration of statin, which might attribute to their better bioavailability. Brain edema defined as an increase in the water content of brain tissue is observed in acute and delayed stages after ICH. Several studies suggest a close association between the degree of perihematomal brain edema and poor outcome in patients.[36,37] Our results showed significantly reduced brain water content of the ipsilateral basal ganglia in the nanomicelle group, at 72 hours after ICH-induction (compared to vehicle). The aforementioned findings support our first hypothesis that rosuvastatin-loaded nanomicelles ameliorate behavioral and morphological outcomes (brain edema) after ICH in mice.

Neuron Degeneration

The degeneration of neurons was next monitored with FJC staining. On the first day, a large number of positive FJC cells were observed in three groups (n=4 per group), and then the number of FJC-positive cells increased to day 3 and then decreased to day 7 after ICH (Figure 5A). Compared to the Vehicle group and the Rosuvastatin group, the number of positive FJC cells in the nanomicell group decreased significantly on day 3 ($p<0.001$) and 7 ($p<0.05$) after ICH (Figure 5B).

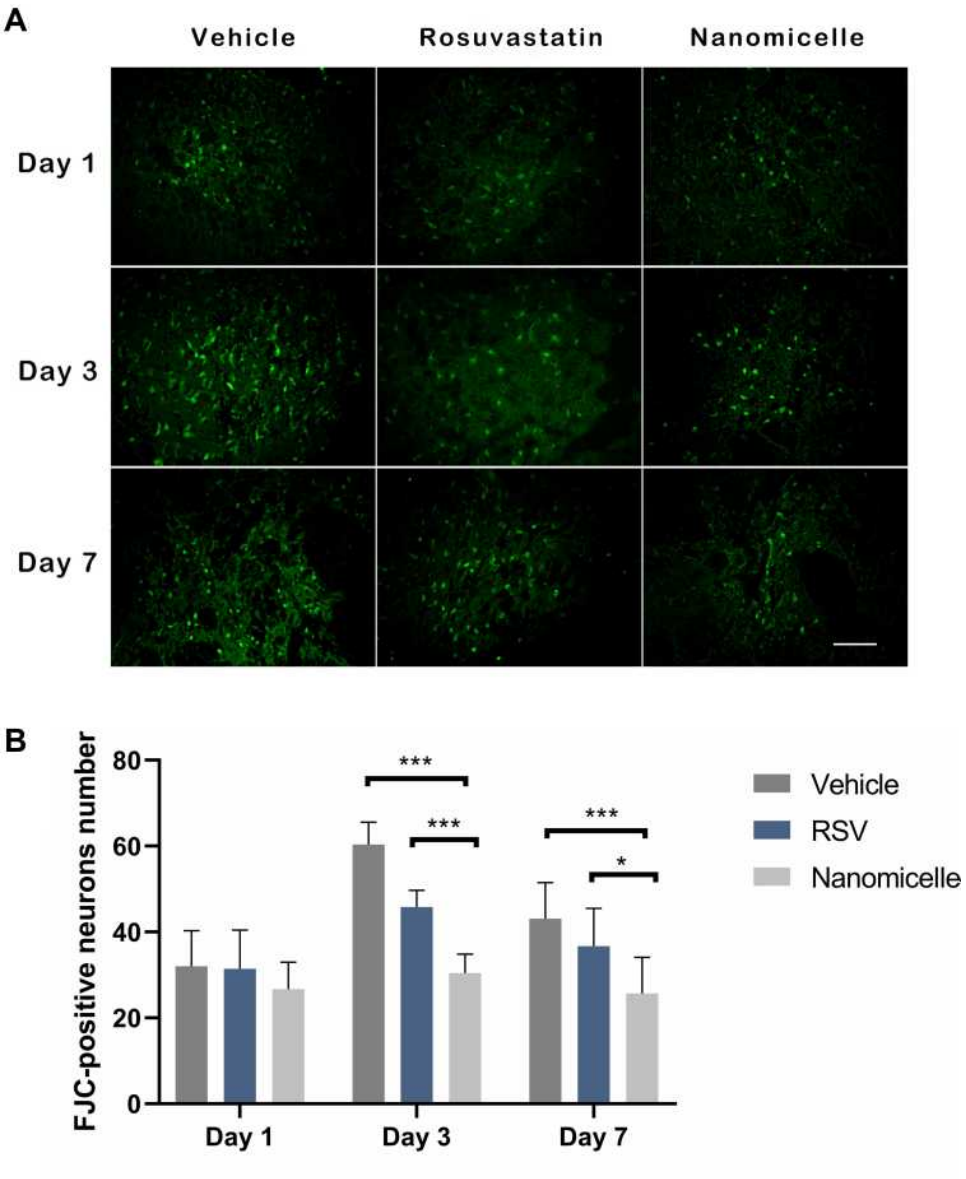

Figure 5 The FJC staining for degenerative neurons. (**A**) Representative images for FJC staining, scale bar = 50μm. (**B**) The statistical analysis of the FJC positive cells. Data are shown as mean ± SD (n = 4), *P < 0.05, ***P < 0.001.

After ICH, apoptotic neurons and astrocytes could be observed from 4 hours to 4 weeks.[38] FJC is a polyanionic fluorescein derivative that sensitively and specifically binds to degenerating neurons.[39] Consistent with the above neurobehavioral outcomes, the results in Figure 5 show that the nanomicelles significantly reduce ICH associated neuron degeneration, hich might explain in part the significant improved neurological deficit in the nanomicelles group, demonstrating that rosuvastatin-loaded nanomicelles displayed greater neuroprotective effects than oral rosuvastatin in ICH mice.

Histopathologic Analysis

To assess the effects of rosuvastatin-loaded nanomicelles on inflammatory cell infiltration, the brain tissues at 1, 3, and 7 day were obtained and H&E staining was employed to detect the pathological changes. As shown in Figure 6, neutrophils were present in the peri-hematoma area as early as 1 day following the hemorrhage. Consistent with previous reports, the activation of microglia/macrophages occurs early in the timeline of neuroinflammation following ICH. At 3 days, increased inflammatory infiltration was observed. Especially in the Vehicle group, a large number of inflammatory cells including neutrophils and

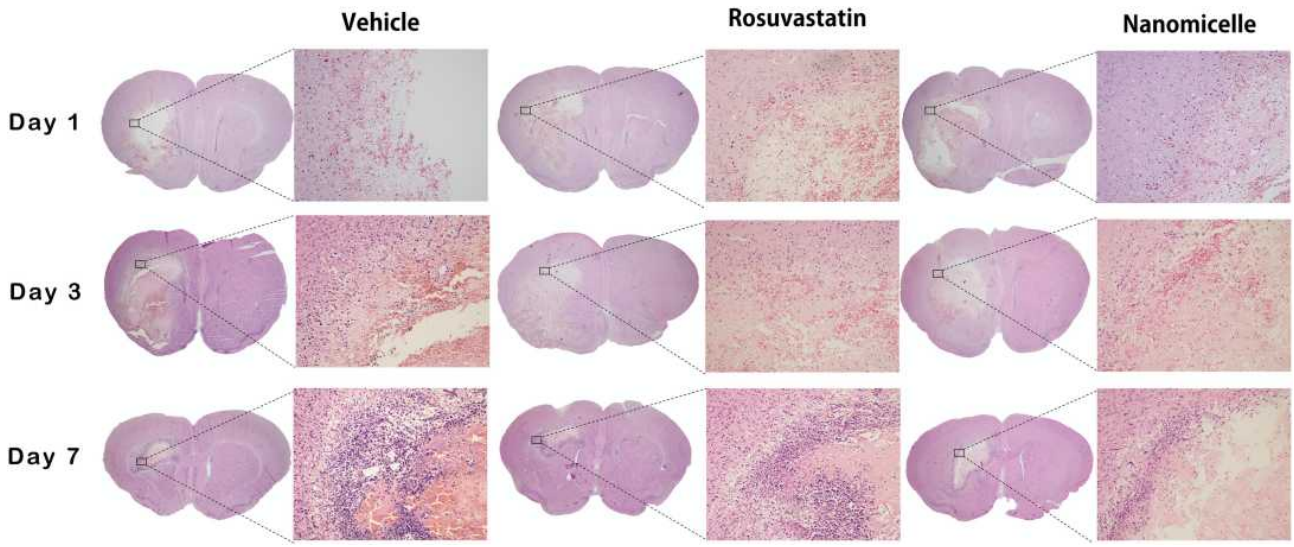

Figure 6 H&E staining. The overall morphology of the brain section at different time-point. Magnified images shows the surrounding of the lesion. Scale bar = 100 μm.

macrophages surrounded and infiltrated the lesion, while there were fewer inflammatory cells appear in the nanomicelles group and Rosuvastatin group. Also, fewer inflammatory cells were observed in the nanomicelles group than that in the Rosuvastatin group. This trend continued to day 7.

Microglia, as one of the primary inflammatory participants, becomes actively involved and phagocytic within a few minutes of the initial bleeding.[40] Besides, activation of the peripheral immune system allows leukocytes to migrate via the broken BBB into the damaged site[41] In the initiation and development of inflammatory reactions, these immune cells play a central role. The degree of recruitment and infiltration of immune cells depends on the concentration of chemokines and BBB permeability. Several reports have shown that statin treatment may decrease inflammatory cell infiltration in the ICH boundary zone.[3,42,43] Here, the nanomicelles proved more effective in inhibiting the inflammatory cell infiltration than oral administration of rosuvastatin.

Microglia Polarization

To evaluate the regulatory effect of the rosuvastatin-loaded nanomicelles on the microglia polarization, Brain sections were immunostained for iNOS/Iba-1 (M1-like marker) or Arginase/Iba-1 (M2-like marker).[44] On days 1, 3, and 7, massively activated microglia were observed to surround hematoma (Figure 7A and B), and the number of microglia (Iba-1$^+$) cells progressively increased over time. As shown in Figure S1 A, B (Supplementary data), the percentage of iNOS$^+$ Iba-1$^+$ cells/Iba-1+ cells was significantly decreased in the Nanomicelle group compared to that in the Vehicle group ($p<0.001$) and Rosuvastatin group ($p<0.001$) at 3 days post-ICH. This difference persisted at 7 days. In contrast, on day 3 and 7, nanomicelle treatment increased percentage of Arg-1$^+$ Iba-1$^+$ cells/Iba-1$^+$ cells compared with Vehicle group ($p<0.01$) and Rosuvastatin group ($p<0.01$). Also, Western blot analysis was carried out and iNOS, ARG-1 expression was determined (Figure 7C and D). In nanomicelle group, iNOS expression reduced at day 3 ($p<0.05$) and ARG-1 expression was increased at day 7 ($p<0.01$) compare with vehicle group. However, no significant difference was observed between the rosuvastatin group and vehicle group.

According to the microenvironment, microglia can adopt two phenotypes: classically (M1) or (M2) activated microglia. M2-like microglia secretes anti-inflammatory cytokines, such as IL-10, and contributes to the hematoma absorption, tissue healing, and repair; however, M1-like microglia increases proinflammatory cytokines, aggravating brain injury including BBB damage, brain edema, oxidative stress reaction.[40] Earlier studies suggested that statins decreased the infiltration of the CNS by promoting a shift in Th1/Th2 balance toward the Th2 phenotype.[45,46] Subsequent studies demonstrated that statins regulated the activation and differentiation of microglia in many CNS disorders and insults.[47] A previous study noted that simvastatin treatment accelerated M2 phenotype polarization after ICH.[33] Similarly, we observed that rosuvastatin-loaded nanomicelle promoted the polarization of microglia/macrophages to M2 phenotype, and this effect could

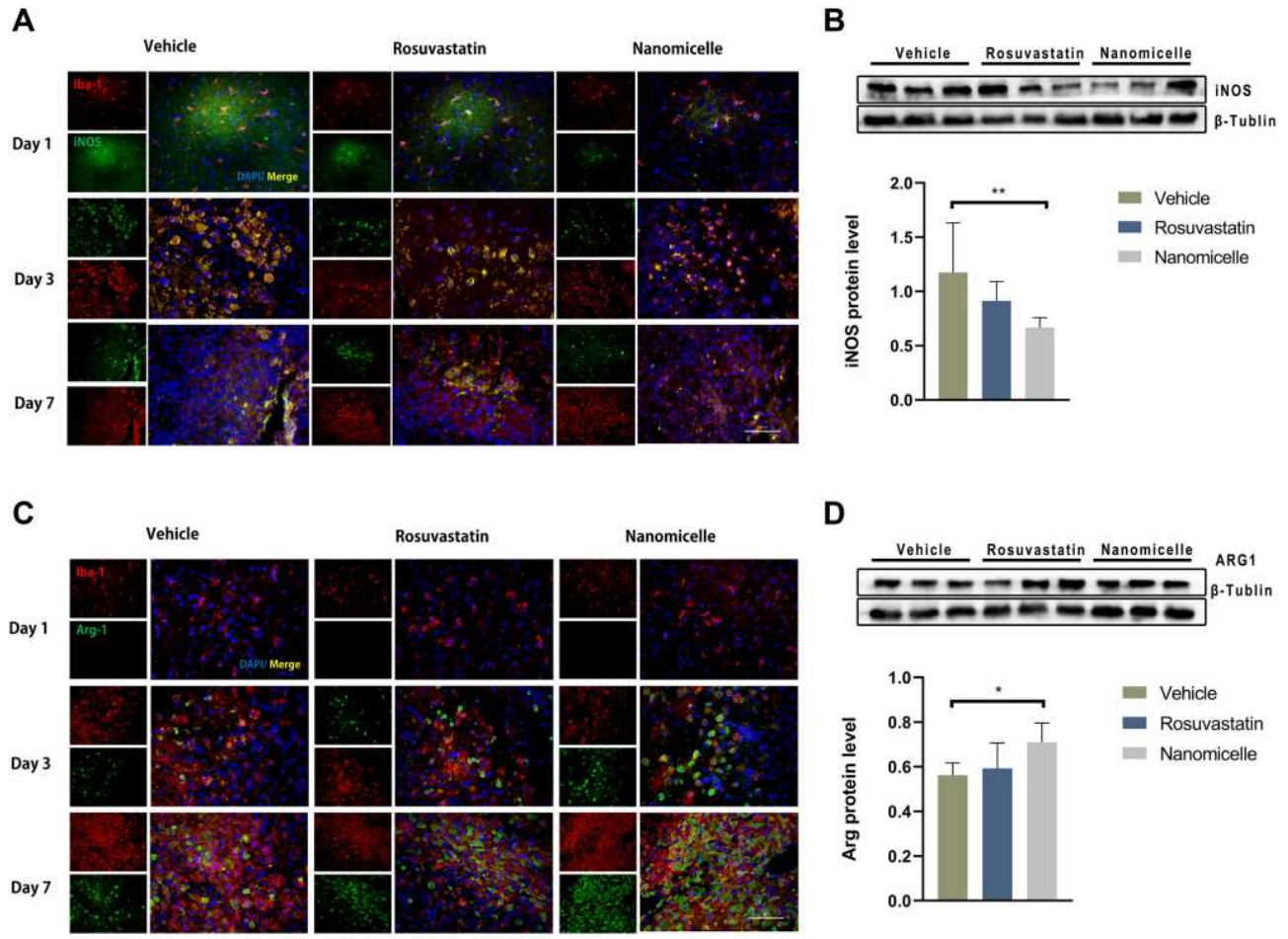

Figure 7 The effects of nanomicelle on Microglia/macrophages polarization. (**A**) Immunofluorescence staining of iNOS+Iba-1+ around the hematoma border zone. (**B**) Western blot analysis of iNOS protein. (**C**) Immunofluorescence staining of Arg-1+Iba-1+ around the hematoma border zone. (**D**) Western blot analysis of iNOS protein. Scale bar =100μm. Data are mean ± SD, n = 6 mice per group, *P < 0.05, **P<0.01.

be explained by the putative anti-inflammatory and immunomodulatory effects of statins. Growing evidence suggested that microglial function modulation may be estimated to lower brain damage associated with ICH, thereby facilitating tissue regeneration and functional recovery.[40]

The Effect of Nanomicelles in vitro Macrophage Cells

To further ascertain that rosuvastatin-loaded nanomicelles possess the same functionality as that of intact statin, we undertook an in vitro approach. RAW 264.7 cells were pretreated with same concentrations of rosuvastatin and rosuvastatin loaded nanomicelle. Subsequently, we stimulated cells by lipopolysaccharide (LPS) and interferon-γ, then analysed the expression of iNOS and ARG-1 protein by immunofluorescence. Macrophages are polarized by microenvironmental signals to distinct functional programs, and L-arginine metabolism is a key aspect in this process as it acts as a substrate for two competing enzymes, iNOS and Arg-1.[48] Consequently, iNOS and Arg-1 were widely used as a macrophage marker polarization marker protein. The results, as shown in Figure 8A–D, indicate that treatment of nanomicelles reduced the iNOS expression and enhanced ARG-1 expression (compare with vehicle group, p<0.01). This is in agreement with the results from animal experiments, described above. It has also been demonstrated that statin-loaded nanomicelles possess the same functionality, even potentially better than as that of intact statin.

Inflammatory Cytokines

Pro-inflammatory cytokines such as IL-1β and TNF-α were determined by immunohistochemical staining. As shown in Figure 9A and B, IL-1β and TNF-α expression

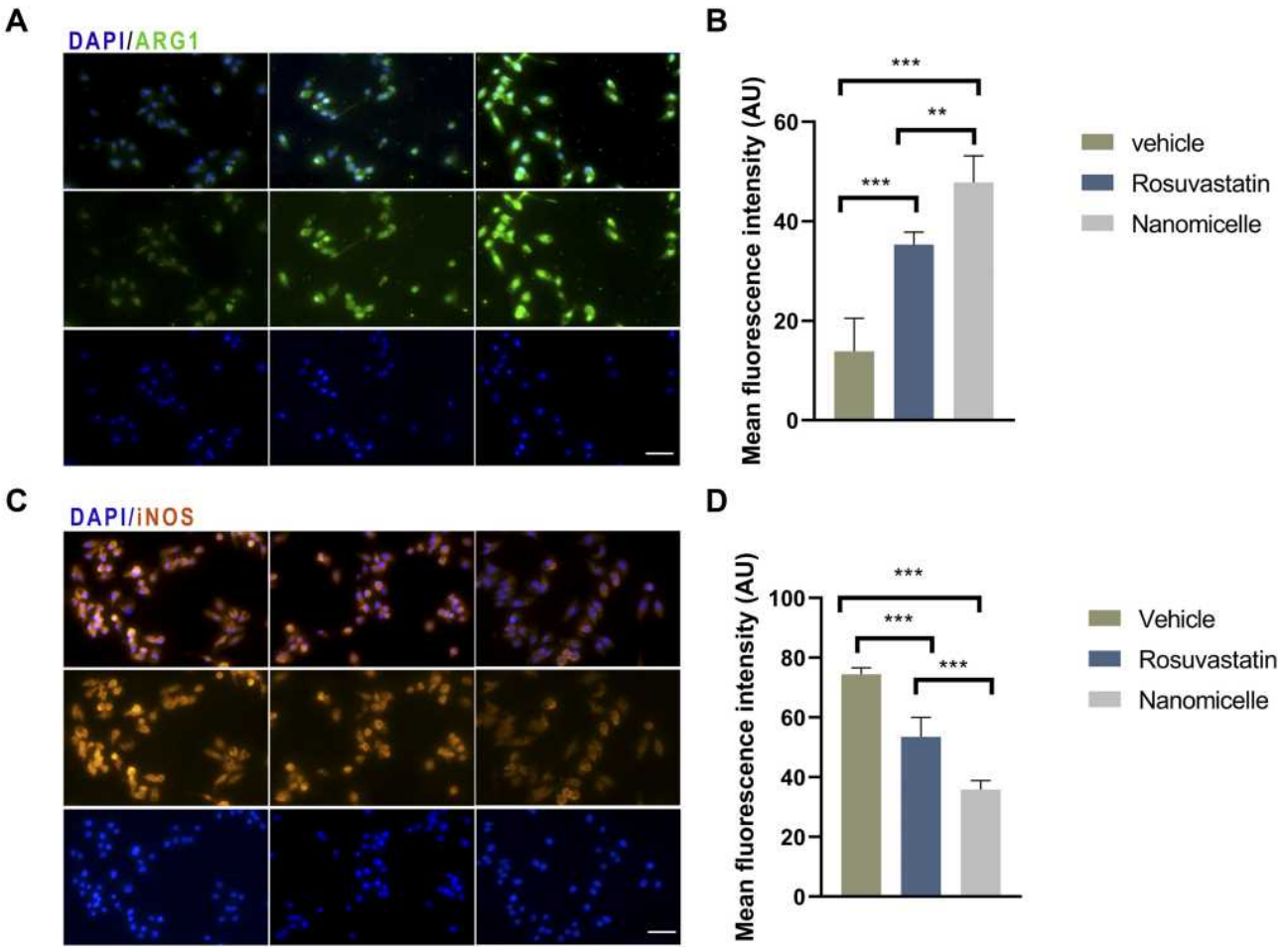

Figure 8 The effects of nanomicelles on RAW 264.7 macrophage cells induced by LPS and INF-γ. (**A**) Immunofluorescence staining of iNOS. (**B**) Measurement of mean fluorescent intensity of INOS. (**C**) ARG-1 immunofluorescence staining. (**D**) Measurement of mean fluorescent intensity of ARG staining. Scar bar = 50μm, **P<0.01, ***P < 0.001.

markedly increased after 1 day following ICH, reached a peak at 3 days, and then gradually decreased to substantially low levels at 7 days. For the nanomicelle group, both the levels of IL-1β and TNF-α significantly decreased compared to those in the vehicle group ($p<0.05$) and the Rosuvastatin group ($p<0.05$) on day 3. When the time prolonged to day 7, both the levels of IL-1β and TNF-α in the nanomicelle group remain significantly decreased compared to those in the Vehicle group ($p<0.05$), while there was no significant difference to that in the Rosuvastatin group, which probably due to both of them in low levels (Figure S2 A, B) (Supplementary data). The corresponding protein expression results of Western blot also confirmed the immunohistochemical results, as indicated in Figure 9C and D. The nanomicelle treatment significantly reduced expression of pro-inflammatory cytokines TNF-a ($p<0.05$) and IL-1 ($p<0.05$) at 3 days post-ICH. Interleukin 10 (IL-10) as an anti-inflammatory cytokine is necessary to maintain a balance between pro-inflammatory and anti-inflammatory processes. As shown in Figure S2 C (Supplementary data), nanomicelle treatment increases IL-10 expression at 7 days post-ICH ($p<0.05$, compare with vehicle group).

Accumulating evidence suggests that after ICH, proinflammatory cytokines are involved in the brain injury phase.[3,4] By promoting the differentiation of microglia/macrophages into the M1-like phenotype, proinflammatory cytokines enhance the release of additional proinflammatory cytokines and downstream transcription factors (Figure 10A).[40] Here, we find that the expression of the downstream inflammatory factors, such as TNF-α and IL-1β, was significantly inhibited by rosuvastatin-loaded micelle. The combination of the above results that the rosuvastatin-loaded micelles promoted the polarization of microglia/macrophages to M2 phenotype, and thus it is reasonable to propose

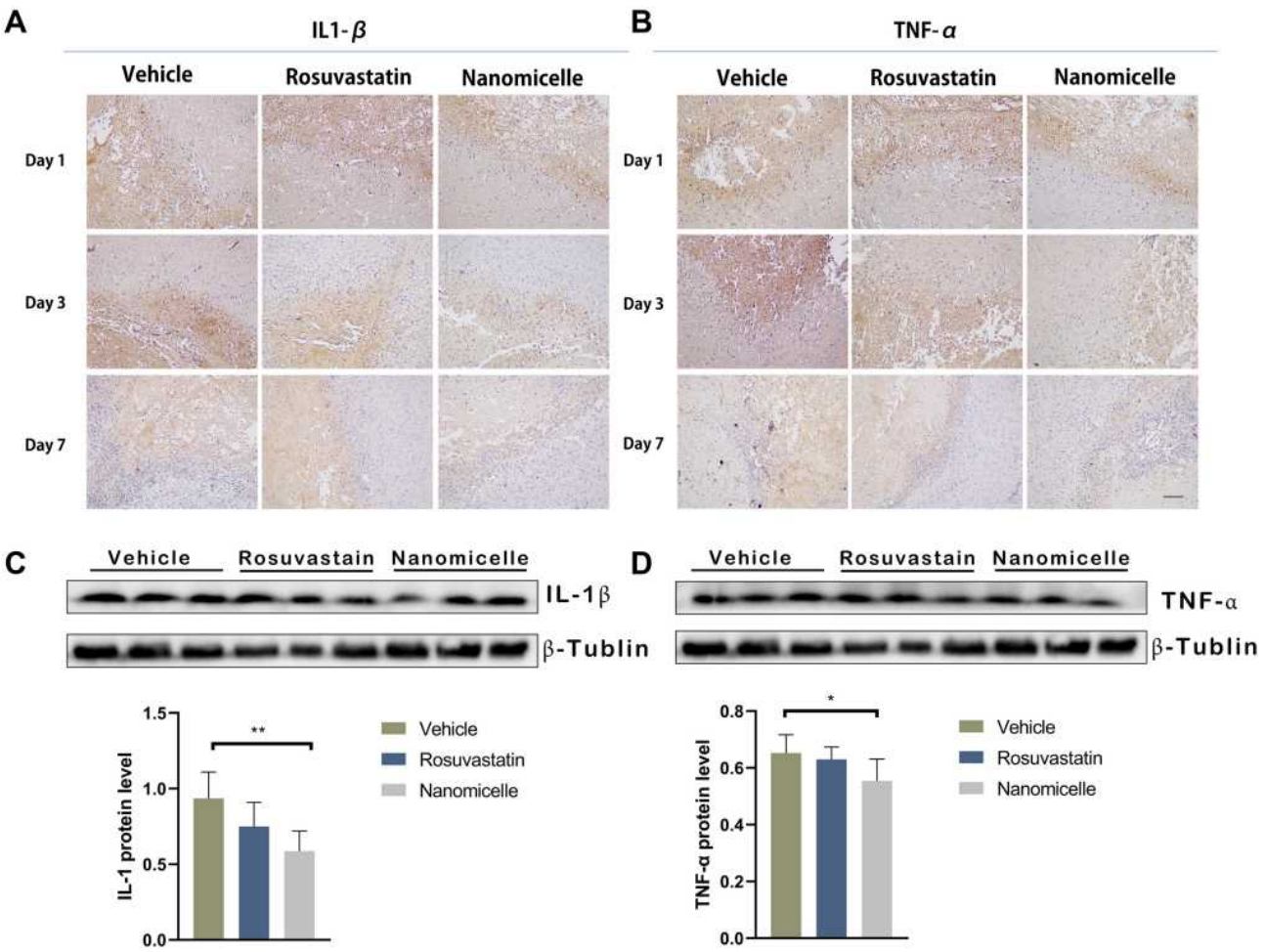

Figure 9 The effects of nanomicelle on pro-inflammatory cytokines in the hematoma border zone. (**A**) Immunohistochemical staining of IL-1β around the hematoma border zone. (**B**) Immunohistochemical staining of TNF-α around the hematoma border zone. (**C**) Western blot analysis of IL-1β. (**D**) Western blot analysis of TNF-α. Data are mean ± SD, n = 6 mice per group, *P < 0.05, **P<0.01. Scale bar =100 μm.

that the micelles down-regulated the expression of the proinflammatory cytokines through promoting M2 phenotype polarization. Although the underlying mechanism is not completely clear, some reasons have been suggested in recent years (Figure 10B). First, statins can inhibit pro-inflammatory cytokines by restricting NFκB-induced transcription factors.[46] By restricting the phosphorylation and expression of STAT-1 and STAT-3, statins can also inhibit pro-inflammatory cytokines such as IL-6 and IL-23 release.[49] Second, statins are capable of amplifying STAT-6, which causes M2 polarization and IL-4 secretion. Meanwhile, statins can also induce SOCS3 and SOCS7 expression to suppress pro-inflammatory cytokines.[50] Statins can also activate anti-inflammatory transcription factor—peroxisome proliferator-activated receptors (PPARs), interfering with NFκB activity.[51]

Conclusion

In conclusion, rosuvastatin-loaded nanomicelles were prepared using a simple solvent evaporation method. The nanomicelles were characterized by TEM, DLS, and cytotoxicity in vitro. Subsequently, the effects of the nanomicelles were assessed in vitro macrophage cells culture and in vivo by an ICH mouse model. The results showed that the nanomicelles could inhibit the inflammatory cell infiltration, reduce the brain edema, modulate microglia/macrophage polarization, decrease the expression of IL-1b and TNF-a, increase the expression of IL-10, reduce the neuron degeneration, and thus promote the nerve functional recovery. Overall, using nanomicelles to deliver statin could be the potential to target the neuroinflammation and improve its efficacy in ICH therapy.

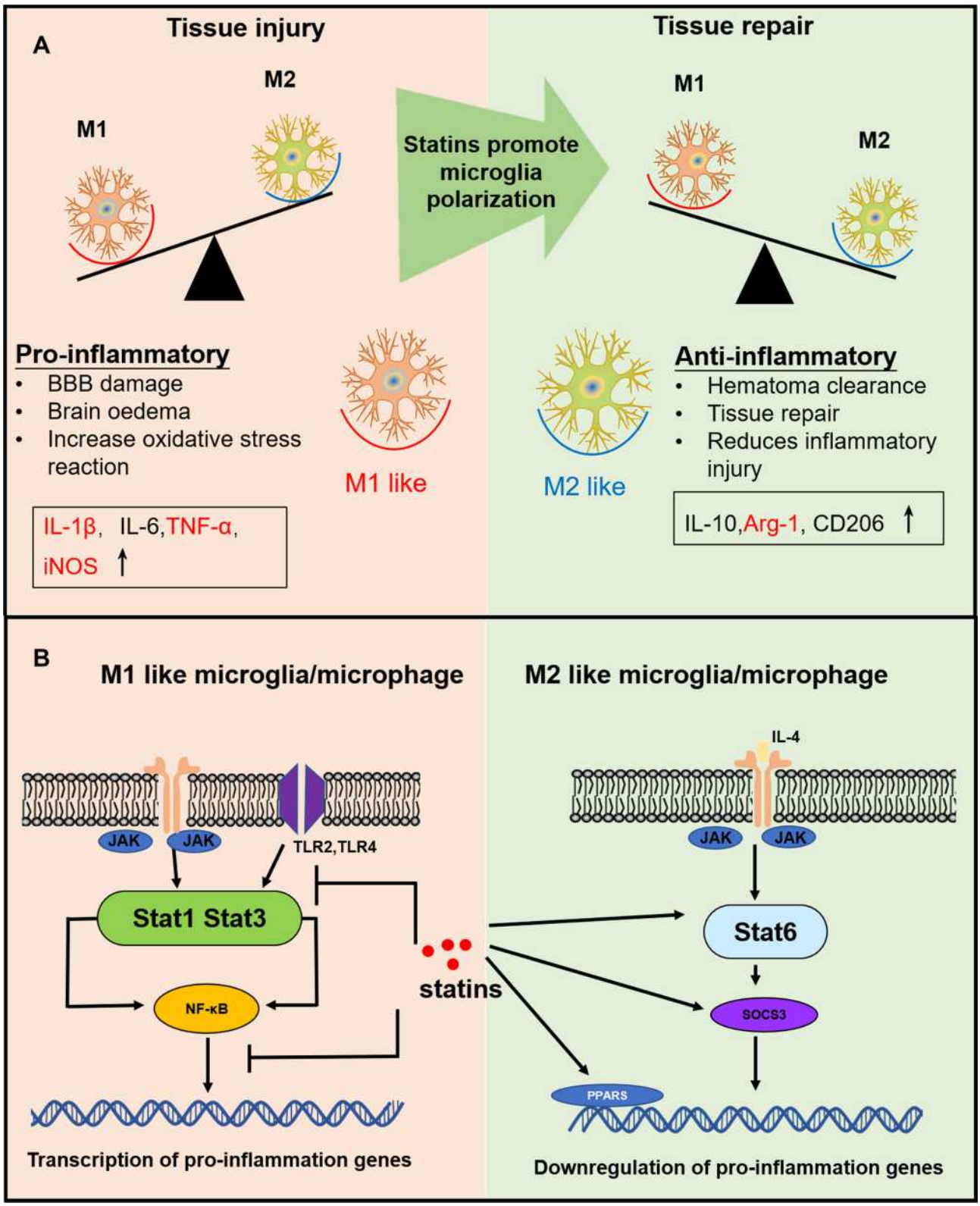

Figure 10 (**A**) The effects of differentially polarized microglia on intracerebral hemorrhage-induced secondary brain injury. (**B**) Possible anti-inflammation mechanism of statins.

Abbreviations

ICH, Intracerebral hemorrhage; HMGCR, 3-hydroxy-3-methylglutaryl coenzyme A reductase; PEG-PCL, poly (ethylene glycol)-block-poly (ε-caprolactone); LDL, lowering low-density lipoprotein; PFA, paraformaldehyde; FJC, Fluoro-Jade C; CCK8, Cell counting kit-8; PDI, polymer dispersity index; DLS, dynamic light scattering; TEM, transmission electron microscopy; NDS, neurologic deficit scale; CNS, central nervous system; H&E, hematoxylin and eosin; PPARs, peroxisome proliferator-activated receptors; LPS, lipopolysaccharide.

Acknowledgment

The authors acknowledge the financial support from the funding of Chengdu Science and Technology Bureau (No. 2019-YF05-00511-SN), and 1.3.5 project for disciplines of excellence, West China Hospital, Sichuan University (ZYJC18007). The authors would like to thank LQ Sima for drawing Figure 1.

Disclosure

The authors report no conflicts of interest in this work.

References

1. van Asch CJ, Luitse MJ, Rinkel GJ, van der Tweel I, Algra A, Klijn CJ. Incidence, case fatality, and functional outcome of intracerebral haemorrhage over time, according to age, sex, and ethnic origin: a systematic review and meta-analysis. *Lancet Neurol*. 2010;9(2):167–176. doi:10.1016/S1474-4422(09)70340-0
2. Cordonnier C, Demchuk A, Ziai W, Anderson CS. Intracerebral haemorrhage: current approaches to acute management. *Lancet*. 2018;392(10154):1257–1268. doi:10.1016/S0140-6736(18)31878-6
3. Zhu H, Wang Z, Yu J, et al. Role and mechanisms of cytokines in the secondary brain injury after intracerebral hemorrhage. *Prog Neurobiol*. 2019;178:101610.
4. Zhou Y, Wang Y, Wang J, Anne Stetler R, Yang QW. Inflammation in intracerebral hemorrhage: from mechanisms to clinical translation. *Prog Neurobiol*. 2014;115:25–44.
5. Sabatine MS, Giugliano RP, Keech AC, et al. Evolocumab and clinical outcomes in patients with cardiovascular disease. *N Engl J Med*. 2017;376(18):1713–1722. doi:10.1056/NEJMoa1615664
6. Li GM, Zhao J, Li B, et al. The anti-inflammatory effects of statins on patients with rheumatoid arthritis: a systemic review and meta-analysis of 15 randomized controlled trials. *Autoimmun Rev*. 2018;17(3):215–225. doi:10.1016/j.autrev.2017.10.013
7. Satoh M, Takahashi Y, Tabuchi T, et al. Cellular and molecular mechanisms of statins: an update on pleiotropic effects. *Clin Sci (Lond)*. 2015;129(2):93–105. doi:10.1042/CS20150027
8. Zhang Q, Dong J, Yu Z. Pleiotropic use of statins as non-lipid-lowering drugs. *Int J Biol Sci*. 2020;16(14):2704–2711. doi:10.7150/ijbs.42965
9. White CM. A review of the pharmacologic and pharmacokinetic aspects of rosuvastatin. *J Clin Pharmacol*. 2002;42(9):963–970. doi:10.1177/009127002401102876
10. Kobayashi M, Chisaki I, Narumi K, et al. Association between risk of myopathy and cholesterol-lowering effect: a comparison of all statins. *Life Sci*. 2008;82(17–18):969–975. doi:10.1016/j.lfs.2008.02.019
11. Chrysant SG. New onset diabetes mellitus induced by statins: current evidence. *Postgrad Med*. 2017;129(4):430–435. doi:10.1080/00325481.2017.1292107
12. Pandit AK, Kumar P, Kumar A, Chakravarty K, Misra S, Prasad K. High-dose statin therapy and risk of intracerebral hemorrhage: a meta-analysis. *Acta Neurol Scand*. 2016;134(1):22–28. doi:10.1111/ane.12540
13. Lin HP, Tu HP, Hsieh YP, Lee BS. Controlled release of lovastatin from poly(lactic-co-glycolic acid) nanoparticles for direct pulp capping in rat teeth. *Int J Nanomedicine*. 2017;12:5473–5485. doi:10.2147/IJN.S138410
14. Tai IC, Wang YH, Chen CH, Chuang SC, Chang JK, Ho ML. Simvastatin enhances Rho/actin/cell rigidity pathway contributing to mesenchymal stem cells' osteogenic differentiation. *Int J Nanomedicine*. 2015;10:5881–5894. doi:10.2147/IJN.S84273
15. Chen J, Jiang Z, Xu W, et al. Spatiotemporally targeted nanomedicine overcomes hypoxia-induced drug resistance of tumor cells after disrupting neovasculature. *Nano Lett*. 2020;20(8):6191–6198. doi:10.1021/acs.nanolett.0c02515
16. Li D, Zhang R, Liu G, Kang Y, Wu J. Redox-responsive self-assembled nanoparticles for cancer therapy. *Adv Healthc Mater*. 2020;9(20):e2000605. doi:10.1002/adhm.202000605
17. Wang L, You X, Dai C, Tong T, Wu J. Hemostatic nanotechnologies for external and internal hemorrhage management. *Biomater Sci*. 2020;8(16):4396–4412. doi:10.1039/D0BM00781A
18. Ding J, Chen J, Gao L, et al. Engineered nanomedicines with enhanced tumor penetration. *Nano Today*. 2019;29.
19. Feng X, Xu W, Li Z, Song W, Ding J, Chen X. Immunomodulatory Nanosystems. *Adv Sci (Weinh)*. 2019;6(17):1900101. doi:10.1002/advs.201900101
20. Han S, Huang K, Gu Z, Wu J. Tumor immune microenvironment modulation-based drug delivery strategies for cancer immunotherapy. *Nanoscale*. 2020;12(2):413–436. doi:10.1039/C9NR08086D
21. Wu C, Xu Q, Chen X, Liu J. Delivery luteolin with folacin-modified nanoparticle for glioma therapy. *Int J Nanomedicine*. 2019;14:7515–7531. doi:10.2147/IJN.S214585
22. Wang Y, Xie J, Ai Z, Su J. Nobiletin-loaded micelles reduce ovariectomy-induced bone loss by suppressing osteoclastogenesis. *Int J Nanomedicine*. 2019;14:7839–7849. doi:10.2147/IJN.S213724
23. Yang L, Zhang Z, Hou J, et al. Targeted delivery of ginsenoside compound K using TPGS/PEG-PCL mixed micelles for effective treatment of lung cancer. *Int J Nanomedicine*. 2017;12:7653–7667. doi:10.2147/IJN.S144305
24. Lin H, Wang Q, Zhong R, et al. Biomimetic phosphorylcholine strategy to improve the hemocompatibility of pH-responsive micelles containing tertiary amino groups. *Colloids Surf B Biointerfaces*. 2019;184:110545. doi:10.1016/j.colsurfb.2019.110545
25. Zhou W, Zi L, Cen Y, You C, Tian M. Copper sulfide nanoparticles-incorporated hyaluronic acid injectable hydrogel with enhanced angiogenesis to promote wound healing. *Front Bioeng Biotechnol*. 2020;8:417. doi:10.3389/fbioe.2020.00417
26. Karki K, Knight RA, Han Y, et al. Simvastatin and atorvastatin improve neurological outcome after experimental intracerebral hemorrhage. *Stroke*. 2009;40(10):3384–3389. doi:10.1161/STROKEAHA.108.544395
27. Xu J, Duan Z, Qi X, et al. Injectable gelatin hydrogel suppresses inflammation and enhances functional recovery in a mouse model of intracerebral hemorrhage. *Front Bioeng Biotechnol*. 2020;8:785. doi:10.3389/fbioe.2020.00785
28. Fang H, Chen J, Lin S, et al. CD36-mediated hematoma absorption following intracerebral hemorrhage: negative regulation by TLR4 signaling. *J Immunol*. 2014;192(12):5984–5992. doi:10.4049/jimmunol.1400054

29. Krafft PR, Altay O, Rolland WB, et al. α7 nicotinic acetylcholine receptor agonism confers neuroprotection through GSK-3β inhibition in a mouse model of intracerebral hemorrhage. *Stroke*. 2012;43(3):844–850. doi:10.1161/STROKEAHA.111.639989
30. Duan Z, Li H, Qi X, et al. Crocin attenuation of neurological deficits in a mouse model of intracerebral hemorrhage. *Brain Res Bull*. 2019;150:186–195. doi:10.1016/j.brainresbull.2019.05.023
31. Kapur NK, Musunuru K. Clinical efficacy and safety of statins in managing cardiovascular risk. *Vasc Health Risk Manag*. 2008;4(2):341–353. doi:10.2147/VHRM.S1653
32. Chen Q, Shi X, Tan Q, et al. Simvastatin promotes hematoma absorption and reduces hydrocephalus following intraventricular hemorrhage in part by upregulating CD36. *Transl Stroke Res*. 2017;8(4):362–373. doi:10.1007/s12975-017-0521-y
33. Wang Y, Chen Q, Tan Q, et al. Simvastatin accelerates hematoma resolution after intracerebral hemorrhage in a PPARγ-dependent manner. *Neuropharmacology*. 2018;128:244–254. doi:10.1016/j.neuropharm.2017.10.021
34. Bouët V, Freret T, Toutain J, Divoux D, Boulouard M, Schumann-Bard P. Sensorimotor and cognitive deficits after transient middle cerebral artery occlusion in the mouse. *Exp Neurol*. 2007;203(2):555–567. doi:10.1016/j.expneurol.2006.09.006
35. Wang YC, Wang PF, Fang H, Chen J, Xiong XY, Yang QW. Toll-like receptor 4 antagonist attenuates intracerebral hemorrhage-induced brain injury. *Stroke*. 2013;44(9):2545–2552. doi:10.1161/STROKEAHA.113.001038
36. Witsch J, Al-Mufti F, Connolly ES, et al. Statins and perihemorrhagic edema in patients with spontaneous intracerebral hemorrhage. *Neurology*. 2019;92(18):e2145–e2149. doi:10.1212/WNL.0000000000006931
37. Selim M, Norton C. Perihematomal edema: implications for intracerebral hemorrhage research and therapeutic advances. *J Neurosci Res*. 2020;98(1):212–218. doi:10.1002/jnr.24372
38. Matsushita K, Meng W, Wang X, et al. Evidence for apoptosis after intercerebral hemorrhage in rat striatum. *J Cereb Blood Flow Metab*. 2000;20(2):396–404. doi:10.1097/00004647-200002000-00022
39. Ehara A, Ueda S. Application of Fluoro-Jade C in acute and chronic neurodegeneration models: utilities and staining differences. *Acta Histochem Cytochem*. 2009;42(6):171–179. doi:10.1267/ahc.09018
40. Lan X, Han X, Li Q, Yang QW, Wang J. Modulators of microglial activation and polarization after intracerebral haemorrhage. *Nat Rev Neurol*. 2017;13(7):420–433.
41. Mracsko E, Veltkamp R. Neuroinflammation after intracerebral hemorrhage. *Front Cell Neurosci*. 2014;8:388. doi:10.3389/fncel.2014.00388
42. Jung KH, Chu K, Jeong SW, et al. HMG-CoA reductase inhibitor, atorvastatin, promotes sensorimotor recovery, suppressing acute inflammatory reaction after experimental intracerebral hemorrhage. *Stroke*. 2004;35(7):1744–1749. doi:10.1161/01.STR.0000131270.45822.85
43. Ewen T, Qiuting L, Chaogang T, et al. Neuroprotective effect of atorvastatin involves suppression of TNF-α and upregulation of IL-10 in a rat model of intracerebral hemorrhage. *Cell Biochem Biophys*. 2013;66(2):337–346. doi:10.1007/s12013-012-9453-z
44. Lan X, Han X, Li Q, et al. Pinocembrin protects hemorrhagic brain primarily by inhibiting toll-like receptor 4 and reducing M1 phenotype microglia. *Brain Behav Immun*. 2017;61:326–339. doi:10.1016/j.bbi.2016.12.012
45. Youssef S, Stüve O, Patarroyo JC, et al. The HMG-CoA reductase inhibitor, atorvastatin, promotes a Th2 bias and reverses paralysis in central nervous system autoimmune disease. *Nature*. 2002;420(6911):78–84. doi:10.1038/nature01158
46. Cheng SM, Lai JH, Yang SP, et al. Modulation of human T cells signaling transduction by lovastatin. *Int J Cardiol*. 2010;140(1):24–33. doi:10.1016/j.ijcard.2008.10.044
47. Bagheri H, Ghasemi F, Barreto GE, Sathyapalan T, Jamialahmadi T, Sahebkar A. The effects of statins on microglial cells to protect against neurodegenerative disorders: a mechanistic review. *Biofactors*. 2020;46(3):309–325. doi:10.1002/biof.1597
48. Baldanta S, Fernández-Escobar M, Acín-Perez R, et al. ISG15 governs mitochondrial function in macrophages following vaccinia virus infection. *PLoS Pathog*. 2017;13(10):e1006651. doi:10.1371/journal.ppat.1006651
49. Zhang X, Jin J, Peng X, Ramgolam VS, Markovic-Plese S. Simvastatin inhibits IL-17 secretion by targeting multiple IL-17-regulatory cytokines and by inhibiting the expression of IL-17 transcription factor RORC in CD4+ lymphocytes. *J Immunol*. 2008;180(10):6988–6996. doi:10.4049/jimmunol.180.10.6988
50. Kagami S, Owada T, Kanari H, et al. Protein geranylgeranylation regulates the balance between Th17 cells and Foxp3+ regulatory T cells. *Int Immunol*. 2009;21(6):679–689. doi:10.1093/intimm/dxp037
51. Dehnavi S, Sohrabi N, Sadeghi M, et al. Statins and autoimmunity: state-of-the-art. *Pharmacol Ther*. 2020;214:107614. doi:10.1016/j.pharmthera.2020.107614